RSC Advances

PAPER

View Article Online
View Journal | View Issue

Cite this: *RSC Adv.*, 2015, **5**, 54978

Metal-free mesoporous carbon nitride catalyze the Friedel–Crafts reaction by activation of benzene†

Qiong Yang,[a] Wenyao Wang,[a] Yanxi Zhao,[a] Junjiang Zhu,*[a] Yujun Zhu[b] and Lihua Wang*[a]

Mesoporous graphitic carbon nitride (mpg-C_3N_4) was synthesized and studied as a metal-free catalyst for Friedel–Crafts acylation of benzene. The synthesis was done by a template method using SiO_2 as template and organic chemicals including guanidine hydrochloride (GndCl), dicyandiamide and urea as precursors. Characterizations by XRD, FT-IR, XPS, N_2 physisorption and TEM indicated that the assumed mpg-C_3N_4 is synthesized irrespective of the precursor used. However, the surface chemistry of mpg-C_3N_4, evaluated from TGA and CO_2-TPD, varied with the precursors and the mass ratio (r) of SiO_2 to precursor. Catalytic results showed that the sample prepared using GndCl as precursor and at mass ratio of SiO_2 to GndCl equals to 0.7, defined as mpg-C_3N_4_$G_{(0.7)}$, exhibits the best activity for the reactions, due to its rich surface basic sites and high surface area. Thus 89% conversion was obtained within 30 min using hexanoyl chloride as electrophile at 90 °C. Even at room temperature (27 °C), 75% conversion can be observed within 30 min. The catalyst is also reusable with *ca.* 80% activities recoverable after washing with ethanol. The excellent catalytic performances, as well as its low cost, straightforward synthesis and metal-free characters, make mpg-C_3N_4_$G_{(0.7)}$ a potential catalyst for Friedel–Crafts acylation of benzene in industry with a "green" route.

Received 12th May 2015
Accepted 16th June 2015

DOI: 10.1039/c5ra08871b

www.rsc.org/advances

1. Introduction

Friedel–Crafts (F–C) are one type of useful and important reactions in organic and fine chemistry, and have been applied in industry for the synthesis of chemical intermediates for more than 100 years. Generally, such reactions are catalyzed by stoichiometric excess amount of acid catalysts, *e.g.*, $AlCl_3$ or $FeCl_3$,[1,2] which however produces large amount of waste (*ca.* 88 wt%) to the environment and is against the strategy of sustainable development.[3] Also, the recycle of the acid catalysts is a challenge for industrial plants. The finding of alternative reagents, which can substitute the current acid catalysts and be recyclable, thus is attractive especially with the more and more strict legislations issued for environmental protection recently.

From the mechanism we know that the role of acid catalysts in the F–C reaction is to activate electrophile participating in the reaction. However, the difficulty of developing sustainable and green acid catalyst for the reaction impels scientists to think if it is possible to catalyze the reaction by activating the nucleophile with a solid base catalyst, in order to avoid the deficiencies of using acid catalysts. Indeed, a recent work by Thomas *et al.* showed that graphitic carbon nitrides (g-C_3N_4), especially those with mesoporous structure (mpg-C_3N_4), can be promising catalysts for such applications through the activation of nucleophile, other than electrophile, due to their large surface areas, rich surface basic sites and the aromatic structure.[4,5] This is interesting as it is different from the traditional way adopted in industrial plants and even that taught in the textbook, where the activation of electrophile is suggested. It thus paves a new vista to conduct the Friedel–Crafts reaction with a "green" route.

The material g-C_3N_4 recently receives great interest in many fields, especially in catalysis, because of its easy synthesis and attractive catalytic performances. It can be facilely prepared by polycondensation of a C-, N-, H- and/or O-containing precursor, such as cyanamide,[6] guanidine hydrochloride (GndCl)[7] and urea,[8] in an inert-gas oven at 550 °C, and because of its polymer character, mesoporous g-C_3N_4 (mpg-C_3N_4) with varied textural structures and surface chemistries can be synthesized by a template method using SiO_2 (ref. 9) or Triton X-100 (ref. 10) as template for example. In catalysis it has been reported that g-C_3N_4 can be a promising catalyst or catalyst's support for various reactions including photocatalytic split of water or degradation of dyes,[11–14] NO decomposition,[15] CO_2 activation,[16,17] Knoevenagel condensations,[18] and selective oxidation

[a]*Key Laboratory of Catalysis and Materials Science of the State Ethnic Affairs & Commission Ministry of Education, South-Central University for Nationalities, Wuhan 430074, China. E-mail: ciaczjj@gmail.com*

[b]*Key Laboratory of Functional Inorganic Material Chemistry, Ministry of Education, School of Chemistry and Materials, Heilongjiang University, Harbin, 150080, China*

† Electronic supplementary information (ESI) available: Data obtained from XRD, FT-IR, XPS, and CO_2-TPD for the supported g-C_3N_4/SiO_2, mpg-C_3N_4 prepared with different precursors, and the fresh/used mpg-C_3N_4_$G_{(0.7)}$, and the activity of mpg-C_3N_4_$G_{(0.7)}$ obtained at different reaction parameters. See DOI: 10.1039/c5ra08871b

or hydrogenation.[19–22] Because of these promising applications, several review articles[23–28] on the catalysis use of g-C_3N_4 have been published recently, demonstrating the great interest of g-C_3N_4 in catalysis. It is generally believed that the surface basic sites of g-C_3N_4 are the active sites of reactions, by providing electrons to activate the adsorbed substrates.

Herein we show that mpg-C_3N_4 with varied degrees of condensation, surface chemistries and surface areas can be obtained by a template (SiO_2) method using different precursors or different mass ratios of SiO_2 to precursor, leading to variations in catalytic performances. The mpg-C_3N_4 prepared using GndCl as precursor and at mass ratio of SiO_2 to GndCl equals to 0.7, mpg-C_3N_4_$G_{(0.7)}$, exhibits the best activity for Friedel–Crafts acylation of benzene with hexanoyl chloride, with 89% and 75% conversion obtained within 30 min at reaction temperature of 90 and 27 °C, respectively. Further, the catalyst can be well recycled and are active for reactions using various electrophiles. The excellent catalytic performances as well as the wide applicability make mpg-C_3N_4 a promising catalyst for "green" activation of benzene by an F–C route.

2. Experimental

2.1. Synthesis of mpg-C_3N_4

4.0 g precursors (dicyandiamide, GndCl or urea) was first balanced and dissolved in 4 mL deionized water by stirring, and the solution was heated to 50 °C (or 80 °C for dicyandiamide). After the precursors were completely dissolved, a given amount of Ludox (28% dispersion) was added dropwise. The mass ratio (r) of SiO_2 to precursor was controlled at 0.4, 0.7 and 1.0, which corresponds to 5.7, 10.0 and 14.3 g Ludox (for dicyandiamide and urea, only $r = 0.7$ was synthesized). After water was evaporated, the resulting white solid was transferred to an air oven and dried at 100 °C overnight, and finally heat-treated in N_2 at 550 °C for 3 h with a heating rate of 3 °C min^{-1}. Depending on the precursor and the mass ratio of silica to precursor, the sample was named as g-C_3N_4/SiO_2_$D_{(0.7)}$, g-C_3N_4/SiO_2_$U_{(0.7)}$ and g-C_3N_4/SiO_2_$G_{(r)}$ (r = 0.4, 0.7, 1.0), where "D", "U" and "G" represent dicyandiamide, urea and GndCl, respectively.

To prepare mesoporous carbon nitride (mpg-C_3N_4), the above obtained composites were treated with 50 mL 4 M NH_4HF_2 for 48 h by drastic stirring to remove the silica template. The powders were then filtrated, washed three times with deionized water and twice with ethanol, and finally dried in a vacuum oven at 50 °C for 6 h. The obtained sample was accordingly named as mpg-C_3N_4_$D_{(0.7)}$, mpg-C_3N_4_$U_{(0.7)}$ and mpg-C_3N_4_$G_{(r)}$ (r = 0.4, 0.7, 1.0), respectively.

2.2. Characterizations

X-ray diffraction (XRD) patterns were collected using a Bruker D8 Advance X-ray diffractometer with Cu Kα (λ = 1.5406 Å) irradiation. FT-IR spectra were collected on a Nicolet 470 FTIR spectrometer, working in the range of 400–4000 cm^{-1} at a resolution of 0.09 cm^{-1}. Thermal gravimetric analysis (TGA) was conducted on a NETZSCH TG 209F3 apparatus. 10 mg samples were first put in an alumina crucible, thereafter air with flow rate of 20 mL min^{-1} was switched on at room temperature. After reaching a stable baseline, the sample was heated from room temperature to 800 °C at a heating rate of 10 °C min^{-1}, to record the profile. Transmission electron microscopy (TEM) images were obtained on a Tecnai G^2 20 S-Twin apparatus with high-resolution transmission electron microscope (200 kV). Before observation the sample was first dispersed in ethanol by ultrasonic method, and then deposited on a copper mesh. N_2 physisorption isotherms were measured on a TriStar II 3020 measurement at liquid nitrogen temperature. Before measurement the sample was treated in vacuum at 150 °C for 5 h. X-ray photoelectron spectroscopy (XPS) spectra were recorded on a VG Multi lab 2000 apparatus using a monochromatic Al Kα X-ray source (300 W) and analyzer pass energy of 25 eV. Binding energies were obtained by referencing to the C (1s) binding energy taken at 284.6 eV.

CO_2-TPD was conducted on a TP-5080 TPD/TPR apparatus (Tianjing Xianquan technology company, China). The sample (80 mg) was first treated in Helium at 150 °C for 1 h and then cooled to room temperature. CO_2 was subsequently switched to the sample for adsorption for 30 min. Thereafter, Helium with flow rate of 30 mL min^{-1} was switched again to the sample, and after reaching a stable baseline, the sample was heated from RT to 400 °C at a rate of 10 °C min^{-1} to record the profile.

2.3. Catalytic tests

The reaction was carried out in a 50 mL three-necked flask, equipped with a water condenser (temperature was controlled at 5 °C). 25 mg catalyst, 0.3 mL benzene, 0.1 mL hexanoyl chloride and 16 mL n-heptane were added to the flask. After the mixture was heated to desired temperature, the reaction was initiated by stirring and the reaction started to count. The reaction mixture was extracted at desired time, centrifuged and analyzed by an Agilent 7890 GC equipped with an FID detector and a HP-5 column. The catalytic activity was evaluated in terms of hexanoyl chloride conversion, as described elsewhere.[4]

3. Results and discussion

Fig. 1A presents the XRD patterns of mpg-C_3N_4 prepared using dicyandiamide, GndCl and urea as precursors. Two characteristic peaks at $2\theta = 12.9°$ and 27.3°, which represent the in-plane structural packing motif and interlayer stacking of aromatic segments, respectively, are observed and can be indexed to the (100) and (002) diffractions of graphitic materials,[29–31] indicating that the mpg-C_3N_4 is prepared. In comparison, the peak intensity of g-C_3N_4 in the g-C_3N_4/SiO_2 composite is largely attenuated, due to the interference of SiO_2 (see Fig. S1A†), and the peak of g-C_3N_4/SiO_2_$U_{(0.7)}$ is even hard to observe, suggesting that the yield or condensation of g-C_3N_4 is different when different precursors are used.

FT-IR spectrum was performed to confirm the formation of g-C_3N_4, Fig. 1B. Based on the classification proposed in literature,[6,32–35] it is known that the band at 805 cm^{-1} and that in the range of 1240–1650 cm^{-1} are attributed to the stretching or

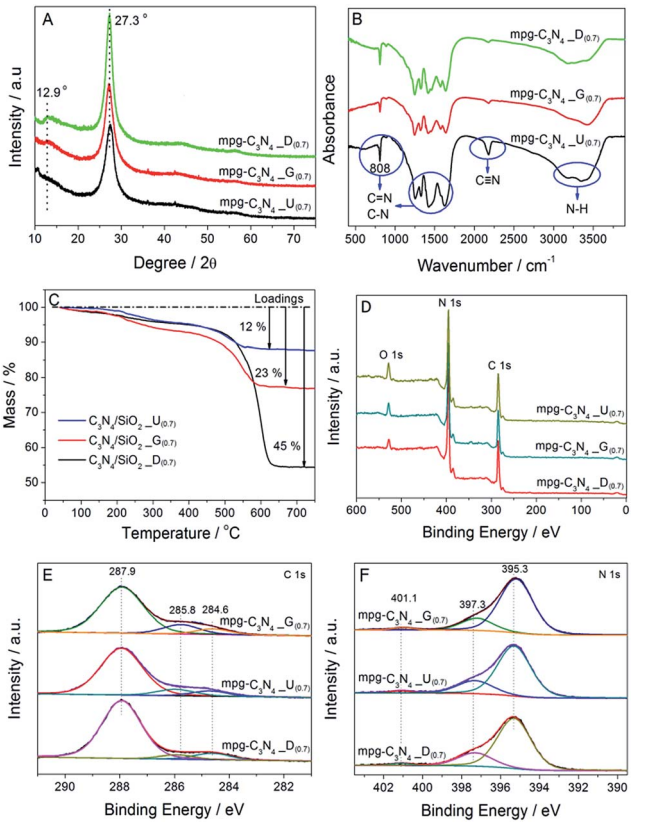

Fig. 1 The physicochemical properties of mpg-C_3N_4 or g-C_3N_4/SiO_2 prepared with different precursors and at mass ratio of SiO_2 to precursor equals to 0.7. (A) Wide angle XRD patterns; (B) FT-IR spectrum; (C) TGA curves; (D)–(F) the total and fine XPS spectra for C 1s and N 1s.

bending vibrations of C–N and/or C=N bonds of the triazine rings, the bands at 3100–3500 cm^{-1} are attributed to the stretching vibrations of N–H bond (=NH or $-NH_2$ group), and the weak band at near 2175 cm^{-1} is to the stretching vibration of C≡N group. The presence of N–H bond indicates that the samples are not fully condensed, and there are =NH or $-NH_2$ groups existing on the edge of g-C_3N_4. These results confirm that the g-C_3N_4 is synthesized. The corresponding IR spectra for g-C_3N_4/SiO_2 composite can be found in Fig. S1B,† in which the absorption peaks attributed to g-C_3N_4, as well as those to SiO_2 (Si–O–Si bond) and –OH groups are observed.

Fig. 1C presents the TGA profiles of the three g-C_3N_4/SiO_2 composites, showing that the loading of g-C_3N_4 prepared with different precursors is different. The loading increases from 12% to 23% and to 45% for samples prepared using urea, GndCl and dicyandiamide as precursor, respectively. This indicates that each precursor undergoes a different polycondensation process and the degree of condensation is different. Urea that contains oxygen atoms in the structure has the possibility of self-combustion during the polycondensation process, yielding CO_2 and/or H_2O, thus has the least g-C_3N_4 loading. GndCl that contains volatile HCl in the structure also leads to low g-C_3N_4 loading as HCl will be released during the polycondensation, without participating in the synthesis process. Dicyandiamide that contains only C, N and H atoms in the structure can be mostly used for the formation of g-C_3N_4, except the essential release of NH_3, thus has the highest g-C_3N_4 loading. This explains why varied g-C_3N_4 loadings are obtained as different precursors are used, and suggests a different polycondensation process among them.

Fig. 1D–F shows the XPS survey spectrum of the three mpg-C_3N_4 samples in the range of 0–600 eV, and the corresponding high-resolution spectrum for C 1s and N 1s. The peaks located at binding energy of 283–290, 392–402 and 525–535 eV can be assigned to the C 1s, N 1s and O 1s, respectively, according to the XPS database. The strong peak intensity of C 1s and N 1s indicates that the materials are composed mainly of C and N atoms. By calculation it is found that the surface molar ratio of C/N atoms is slightly different for the three samples but is near 1 (see Table S1†), which is higher than the theoretical value (0.75), indicating that there are N defects on the surface of samples. The presence of oxygen atoms could be that the samples were contaminated by oxygen when stored in air, and its surface atomic percentage varied from 3.44 to 7.65% (see Table S1†), in sequence of mpg-C_3N_4_$U_{(0.7)}$ > mpg-C_3N_4_$G_{(0.7)}$ > mpg-C_3N_4_$D_{(0.7)}$. The variation in C/N ratios and the different affinities to oxygen imply that the polycondensation process and surface chemistry of samples prepared using different precursors are not the same, which may lead to variations in their catalytic performances as shown below. No peak assignable to Si 2p (97–105 eV) is observed in the spectrum, confirming that the silica is significantly removed from these mesoporous samples and its influence can be neglected in the reaction. In contrast, strong peak intensity of the O 1s and Si 2p is observed for the supported samples (*i.e.*, g-C_3N_4/SiO_2) (see Fig. S2†).

According to literature, three peaks can be fitted for the C 1s and the N 1s spectrum.[36–40] For C 1s, the binding energy at 284.6, 285.8 and 287.9 eV are assigned to the adventitious carbon, the N-bonded sp^3 hybridized C atoms (C–$(N)_3$), and the N-bonded sp^2 hybridized C atoms in an aromatic ring (N–C=N), respectively. For N 1s, the main peak at binding energy of 395.3 eV is attributed to the C–N–C groups, the mediate peak at 397.2 eV is to the N–$(C)_3$ groups, and the weak one at 401.1 eV is to the amino groups carrying hydrogen atoms (C–N–H). It is noted that the peak of tertiary amines is almost 6 times bigger than that of these hydrogen bonded amines, indicating a degree of condensation well beyond the linear polymer melon structure.[39]

Overall, the above results indicate that mpg-C_3N_4 can be prepared using SiO_2 as template, but the polycondensation process and surface properties of them vary with the precursors. To provide more information on the textural structure and surface chemistry, three additional characterizations including TEM, N_2 physisorption and CO_2-TPD were conducted on the selected mpg-C_3N_4_G samples, which showed the best activity in the investigated F–C reactions.

TEM images of the template and the mpg-C_3N_4_$G_{(0.7)}$ are presented in Fig. 2, showing that silica in the Ludox solution is homogeneously dispersed with average particle size of *ca.* 17 nm. As expected, randomly distributed mesoporous pores with pore size of 16 nm are observed for the mpg-C_3N_4_$G_{(0.7)}$, suggesting that the assumed sample is well replicated from the Ludox template.

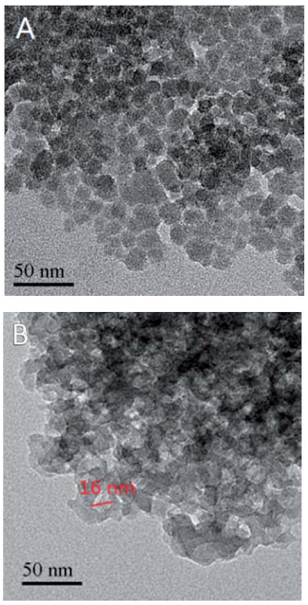

Fig. 2 TEM images for the Ludox template and the replicated mpg-C_3N_4_$G_{(0.7)}$.

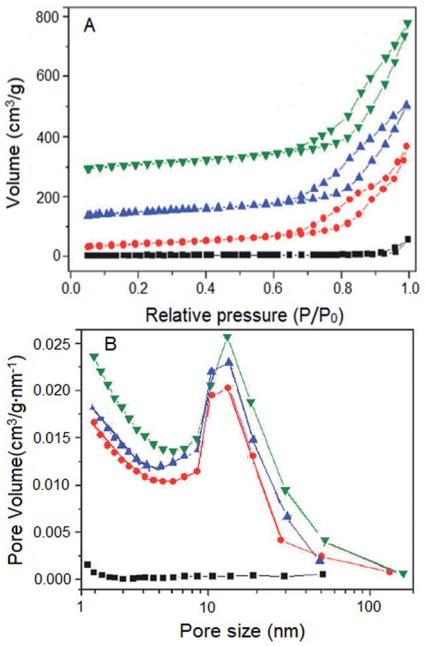

Fig. 3 (A) N_2 physisorption isotherms and (B) pore size distribution of bulk-C_3N_4 (■), mpg-C_3N_4_$G_{(0.4)}$ (●), mpg-C_3N_4_$G_{(0.7)}$ (▲) and mpg-C_3N_4_$G_{(1.0)}$ (▼).

N_2 physisorption isotherms show that a hysteresis loop in the relative pressure of 0.65–1.0, corresponding to a pore size of *ca.* 14 nm, is observed for mpg-C_3N_4_$G_{(0.7)}$, Fig. 3, indicating the formation of mesoporous structure. The pore size is in well consistent with that obtained from the TEM image (16 nm). The hysteresis loop and pore size are almost the same for mpg-C_3N_4_$G_{(r)}$ with varied r values (r = 0.4, 0.7 and 1.0). This is possible as they are prepared with the same template. In contrast, no hysteresis loop and pore is observed for the bulk g-C_3N_4 prepared without template. The corresponding textural data of these samples are listed in Table 1.

The BET surface area for g-C_3N_4 and mpg-C_3N_4_$G_{(r)}$ (r = 0.4, 0.7 and 1.0) is 11, 144, 166 and 151 $m^2\ g^{-1}$, respectively, with the highest value obtained at r = 0.7. The significant increase in the BET surface area from g-C_3N_4 to mpg-C_3N_4_$G_{(r)}$ suggests that pores are created when template is used. The change in the BET surface area of mpg-C_3N_4_$G_{(r)}$ is slightly different from that reported by Wang *et al.*,[9] who used cyanamide as precursor and found that the surface area increases linearly with the mass ratio of silica to cyanamide. The reason could be that the wall thickness of mpg-C_3N_4 prepared with GndCl as precursor is thinner than that prepared with cyanamide, since the former will release HCl as well as NH_3 during the polycondensation process (see also the TGA profiles above), leading to lower loading or thinner layer of g-C_3N_4 on the silica support. Thus the pore wall of mpg-C_3N_4_$G_{(r)}$ would be collapsed during the template leaching process, and this starts to occur at r = 1.0 in the present case. Indeed, it is found that the pore volume of mpg-C_3N_4_$G_{(1.0)}$ is also lower than that of mpg-C_3N_4_$G_{(0.7)}$, confirming that some pore walls are collapsed.

Fig. 4 shows the CO_2-TPD profiles of mpg-C_3N_4_$G_{(r)}$ (r = 0.4, 0.7 and 1.0), with the aim of evaluating the surface basicity of the samples. Two CO_2 desorption peaks locating at 65 and 246 °C are observed for the samples, indicating that there have at least two types of surface basic sites on their surfaces. The peak area, either for the first or the second, decreases with the increase of r (see the data listed in the lower right corner of Fig. 4), while no appreciable change in the peak position is observed, indicating that the intensity of surface basicity of the samples is similar. This is possible as they are prepared and treated with the same manner. The decrease in the surface basic sites could be attributed to a more condensed g-C_3N_4 structure, as is observed for CNx/SBA-15 polycondensed at different temperatures.[41] Therefore, the sample with lower mass loading or prepared at higher mass ratio (r) has the chance of forming more condensed structure, as GndCl is better dispersed at this condition and thus has the possibility of reacting with each other more sufficiently.

Table 1 Textural data of mpg-C_3N_4_$G_{(r)}$ prepared at different r values using GndCl as precursor

Catalyst	BET/$m^2\ g^{-1}$	Pore size/nm	Pore volume/$m^3\ g^{-1}$
Bulk-C_3N_4	11	—	0.03
mpg-C_3N_4_$G_{(0.4)}$	144	14.0	0.55
mpg-C_3N_4_$G_{(0.7)}$	166	14.2	0.62
mpg-C_3N_4_$G_{(1.0)}$	151	14.4	0.61

The CO_2-TPD profiles of mpg-C_3N_4 prepared with different precursors were also measured and compared in Fig. S3,† showing that mpg-C_3N_4_$G_{(0.7)}$ has the biggest peak area for the second CO_2 desorption peak, and the peak area of the first CO_2 desorption peak is slightly smaller than that of mpg-C_3N_4_$U_{(0.7)}$, while no definite CO_2 desorption peak is observed for mpg-C_3N_4_$D_{(0.7)}$, indicating that the surface chemistry is significantly different if different precursors are used. Based on the

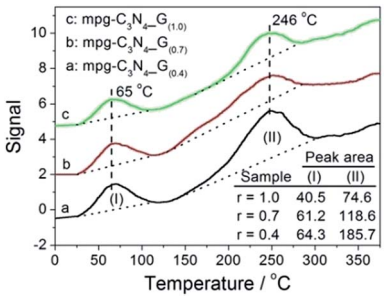

Fig. 4 CO_2 TPD profiles of mpg-C_3N_4_$G_{(r)}$ (r = 0.4, 0.7 and 1.0).

surface structure of g-C_3N_4 proposed in literature[34] it is inferred that the first peak is attributed to the desorption of CO_2 adsorbed on the nitrogen site of C–N–C rings, and the second peak is to the amino groups (–NH and/or ═NH) on the surface edge. On this basis, it can be inferred that sample mpg-C_3N_4_$G_{(0.7)}$ has the most amounts of surface amino groups.

Fig. 5A presents the catalytic performances of mpg-C_3N_4 prepared with various precursors for F–C acylation of benzene with hexanoyl chloride at reaction temperature of 90 °C, showing that the catalysts are active for the reaction, with 89% conversion obtained from mpg-C_3N_4_$G_{(0.7)}$ even at 30 min. By comparison, 78% and 57% conversion are obtained from mpg-C_3N_4_$D_{(0.7)}$ and mpg-C_3N_4_$U_{(0.7)}$, respectively. This indicates that GndCl is the preferred precursor in the preparation of mpg-C_3N_4 used for F–C reaction. The difference in the activities suggests that there is something different in the mpg-C_3N_4 prepared with different precursors. Considering that they all have the g-C_3N_4 phase structure (see Fig. 1), we suspected that the difference among them must be due to the variations in surface chemistry, such as the amount of surface basic sites.

Indeed, by correlating the activity with the amount of surface basic site of mpg-C_3N_4_$G_{(0.7)}$ and mpg-C_3N_4_$U_{(0.7)}$, it can be found that the second CO_2 desorption peak, corresponding to the amount of amino groups on the surface edge, relates intimately to the activity. In a previous work we have reported that the increase of amino groups (induced by doping Zn in the framework) can improve the activity of g-C_3N_4 for NO decomposition due to an enhanced ability for electron transfer.[15] This supports the above observations as the activation of benzene also requires electrons transferred from the catalyst. Consequently, mpg-C_3N_4_$G_{(0.7)}$ with the most surface amino groups showed the best activity for F–C reaction. In the following, we thus chose GndCl as precursor to prepare mpg-C_3N_4 for further investigation.

Blank experiment (without catalyst) shows that 15% conversion can be obtained at 120 min, Fig. 5A, which is far lower than that conducted in the presence of catalyst (89% for mpg-C_3N_4_$G_{(0.7)}$ even at 30 min). This indicates that the reaction proceeds mainly by a heterogeneous catalysis, and is catalyzed by the mpg-C_3N_4 catalyst.

A comparison to the supported sample (g-C_3N_4/SiO_2_$G_{(0.7)}$, abbreviated as "S-C" in Fig. 5B), of which the g-C_3N_4 loading is 23 wt%, shows that the mpg-C_3N_4_$G_{(0.7)}$ exhibits almost double

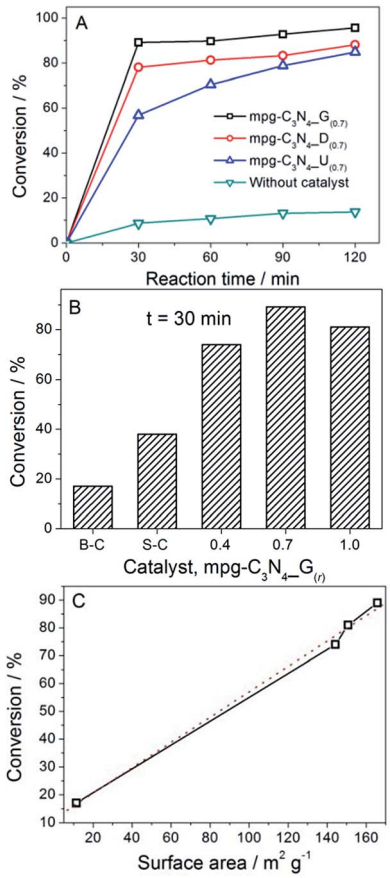

Fig. 5 (A) Conversion obtained from mpg-C_3N_4 prepared with various precursors as a function of reaction time; (B) conversion obtained from bulk g-C_3N_4 (B-C), g-C_3N_4/SiO_2 composites (S-C) and mpg-C_3N_4_$G_{(r)}$ at reaction time of 30 min; (C) an approximate linearly correlation between the BET surface area of catalysts and the conversions of the reaction. Reaction conditions: 25 mg catalyst, 0.3 mL benzene, 0.1 mL hexanoyl chloride and 16 mL n-heptane, temperature: 90 °C.

conversions, Fig. 5B, confirming that it is the g-C_3N_4 that catalyzes the reaction. On the other hand, the g-C_3N_4/SiO_2_$G_{(0.7)}$ shows however higher conversion than the bulk g-C_3N_4 (abbreviated as "B-C" in Fig. 5B), although the mass of g-C_3N_4 in the latter is more. This could be that the former has larger surface area (612 m^2 g^{-1}), which is far higher than that of the latter (11.4 m^2 g^{-1}), thus more surface basic sites can be exposed to the substrates, accelerating the reaction rate. That is, surface area is a crucial parameter determining the catalytic performances of g-C_3N_4 for F–C acylation of benzene with hexanoyl chloride.

To study the influence of surface area on the catalytic performances, mpg-C_3N_4_$G_{(r)}$ with different surface areas but similar pore sizes (to exclude the influence of pore size) were prepared using the same Ludox template but different mass ratios (r) of silica to GndCl. Catalytic tests show that mpg-C_3N_4_$G_{(0.7)}$ with the largest surface area exhibits the highest activity, and bulk g-C_3N_4 with the smallest surface area exhibits the lowest activity, with an order of mpg-C_3N_4_$G_{(0.7)}$ > mpg-C_3N_4_$G_{(1.0)}$ > mpg-C_3N_4_$G_{(0.4)}$ > bulk g-C_3N_4, Fig. 5B, which fits well to the changes in BET surface area listed in Table 1. Indeed,

a correlation between the conversion and the BET surface area shows that the conversion increases almost linearly with the BET surface area, Fig. 5C, pointing out the importance of surface area in determining the reaction activity.

It is noted that the changes in activity and surface basic sites counted from CO_2-TPD measurement are not in the same trend for samples prepared with different mass ratio of SiO_2 to GndCl, although the surface basic sites are believed to be the active site of the reaction. Namely, mpg-C_3N_4_$G_{(0.4)}$ with the most amount of surface basic sites exhibits the lowest activity relative to mpg-C_3N_4_$G_{(0.7)}$ and mpg-C_3N_4_$G_{(1.0)}$. The reason could be that the amount of surface basic sites measured by CO_2 cannot be fully used for the reaction. That is, some surface basic sites (*e.g.*, those in the narrow interspace) that are accessible to CO_2 may not be accessible to benzene, which has larger molecular size (than CO_2), and it seems that only at $r \geq 0.7$ could the surface basic site be mostly used for benzene adsorption.

Because of the high catalytic efficiency of mpg-C_3N_4_$G_{(0.7)}$ at 90 °C, we have the attempt to see if the catalyst has sufficient capability to catalyze the reaction at a low temperature, with the aim of energy savings. Interestingly, we found that no appreciable loss in the conversion is observed at 70 °C (except that at 30 min), and 75% conversion can be achieved even at room temperature (27 °C), Fig. 6A (more can be found in Table S3†) indicating that mpg-C_3N_4_$G_{(0.7)}$ is highly active for the reaction and has the potential of being industrialized. Effects of other reaction conditions including the concentration of substrates, the type of solvents and electrophiles on the reaction are also investigated and the results are listed in Table S2,† showing that (1) the catalyst has good ability to catalyze the reaction even at high concentrations, (2) heptane is the optimized solvent for the reaction and (3) the catalyst is active for the Friedel–Crafts acylation of benzene using varied electrophiles.

In the end, the reusability of mpg-C_3N_4_$G_{(0.7)}$ for the reaction is tested, which is another important parameter in evaluating the possibility of catalyst for industrial use. In each cycle the catalyst was balanced to 25 mg, and the mass of catalyst lost in the filtration process was balanced from a parallel experiment. Fig. 6B shows the conversion obtained within 5 cycles. A half decrease in the conversion is observed when the catalyst is reused directly after the reaction ("0" *vs.* "6"), which could be that (1) the structure of catalyst was destroyed or (2) the active site was blocked (by benzene for example) after the reaction. To check which is the reason accounting for this decrease, we washed the used sample with ethanol several times to extract benzene possibly adsorbed on the catalyst, and then tested its activity again. Results indicate that the activity can be largely recovered after this treatment, thus suggesting that the decreased activity is not attributed to the destruction of catalyst, but to the block of active sites. Indeed, characterizations on the used samples by XRD and FT-IR indicate that the phase structure is not changed and benzene is presented on the surface of the used catalyst, which however can be significantly removed after the ethanol extraction process, see Fig. S4.† Further optimizations on using a more efficient extraction agent to extract benzene from the surface of catalyst, to release the active site, will be done in our forthcoming work, in order to pave the way of industrialization for the catalyst.

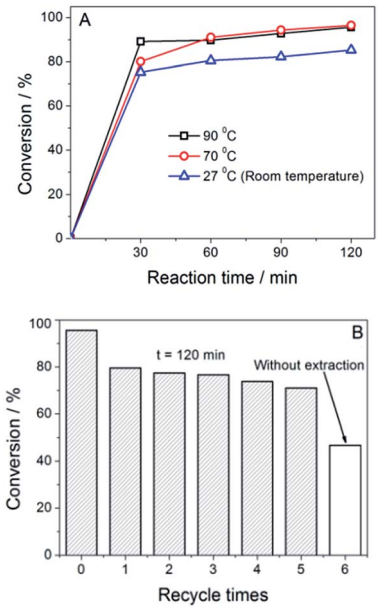

Fig. 6 (A) Conversion obtained from mpg-C_3N_4_$G_{(0.7)}$ at different temperatures; (B) reusability of mpg-C_3N_4_$G_{(0.7)}$ in the Friedel–Crafts acylation of benzene with hexanoyl chloride. Reaction conditions: 25 mg catalyst, 0.3 mL benzene, 0.1 mL hexanoyl chloride and 16 mL *n*-heptane, temperature: 90 °C.

4. Conclusions

In summary, we showed here that mpg-C_3N_4 can be replicated from a Ludox template with various precursors including dicyandiamide, GndCl and urea. The textural and surface properties of mpg-C_3N_4, such as surface area and surface basic sites, can be controlled by using different precursors or changing the mass ratio (r) of template to precursor. Herein, sample prepared using GndCl as precursor and at mass ratio of template to precursor equals to 0.7, mpg-C_3N_4_$G_{(0.7)}$, shows the best activity to F–C acylation of benzene with hexanoyl chloride, with about 75% conversion even at room temperature (27 °C) within 30 min. Also, the catalyst can be well recycled, especially when a suitable agent is used to extract the benzene adsorbed on its surface. The high reactivity at room temperature and the good reusability of mpg-C_3N_4_$G_{(0.7)}$ enable it to be a potential catalyst for the F–C reaction in industrial application.

Acknowledgements

Finance support from the National Science Foundation of China (no. 21203253, 21203254), the Natural Science Foundation of Hubei Province of China (2015CFA138), the Science and Technology Activities of Overseas Personnel Preferential Funding Project (no. BZY14038) and the Key Laboratory of Functional Inorganic Material Chemistry, Ministry of Education, Heilongjiang University, is gratefully appreciated.

Notes and references

1 M. Bandini, A. Melloni and A. Umani-Ronchi, *Angew. Chem., Int. Ed.*, 2004, **43**, 550.
2 S.-L. You, Q. Cai and M. Zeng, *Chem. Soc. Rev.*, 2009, **38**, 2190.
3 J. H. Clark, *Green Chem.*, 1999, **1**, 1.
4 F. Goettmann, A. Fischer, M. Antonietti and A. Thomas, *Angew. Chem., Int. Ed.*, 2006, **45**, 4467.
5 F. Goettmann, A. Fischer, M. Antonietti and A. Thomas, *Chem. Commun.*, 2006, **43**, 4530.
6 M. Groenewolt and M. Antonietti, *Adv. Mater.*, 2005, **17**, 1789.
7 J. Xu, H. T. Wu, X. Wang, B. Xue, Y. X. Li and Y. Cao, *Phys. Chem. Chem. Phys.*, 2013, **15**, 4510.
8 F. Dong, L. Wu, Y. Sun, M. Fu, Z. Wu and S. C. Lee, *J. Mater. Chem.*, 2011, **21**, 15171.
9 X. C. Wang, K. Maeda, X. F. Chen, K. Takanabe, K. Domen, Y. D. Hou, X. Z. Fu and M. Antonietti, *J. Am. Chem. Soc.*, 2009, **131**, 1680.
10 Y. Wang, X. Wang, M. Antonietti and Y. Zhang, *ChemSusChem*, 2010, **3**, 435.
11 Y. Zheng, L. Lin, X. Ye, F. Guo and X. Wang, *Angew. Chem., Int. Ed.*, 2014, **53**, 11926.
12 M. Zhang and X. Wang, *Energy Environ. Sci.*, 2014, **7**, 1902.
13 K. Kailasam, J. D. Epping, A. Thomas, S. Losse and H. Junge, *Energy Environ. Sci.*, 2011, **4**, 4668.
14 H. Xu, J. Yan, Y. Xu, Y. Song, H. Li, J. Xia, C. Huang and H. Wan, *Appl. Catal., B*, 2013, **129**, 182.
15 J. J. Zhu, Y. C. Wei, W. K. Chen, Z. Zhao and A. Thomas, *Chem. Commun.*, 2010, **46**, 6965.
16 F. Goettmann, A. Thomas and M. Antonietti, *Angew. Chem., Int. Ed.*, 2007, **46**, 2717.
17 H. Shi, G. Chen, C. Zhang and Z. Zou, *ACS Catal.*, 2014, **4**, 3637.
18 F. Su, M. Antonietti and X. Wang, *Catal. Sci. Technol.*, 2012, **2**, 1005.
19 P. Zhang, Y. Gong, H. Li, Z. Chen and Y. Wang, *RSC Adv.*, 2013, **3**, 5121.
20 Y. Wang, J. Yao, H. Li, D. Su and M. Antonietti, *J. Am. Chem. Soc.*, 2011, **133**, 2362.
21 J. J. Zhu, S. A. C. Carabineiro, D. Shan, J. L. Faria, Y. J. Zhu and J. L. Figueiredo, *J. Catal.*, 2010, **274**, 207.
22 T. Yuan, H. Gong, K. Kailasam, Y. Zhao, A. Thomas and J. Zhu, *J. Catal.*, 2015, **326**, 38.
23 Y. Wang, X. Wang and M. Antonietti, *Angew. Chem., Int. Ed.*, 2012, **51**, 68.
24 Y. Zheng, J. Liu, J. Liang, M. Jaroniec and S. Z. Qiao, *Energy Environ. Sci.*, 2012, **5**, 6717.
25 X. Wang, S. Blechert and M. Antonietti, *ACS Catal.*, 2012, **2**, 1596.
26 X.-H. Li and M. Antonietti, *Chem. Soc. Rev.*, 2013, **42**, 6593.
27 J. Zhu, P. Xiao, H. Li and S. A. C. Carabineiro, *ACS Appl. Mater. Interfaces*, 2014, **6**, 16449.
28 Y. Gong, M. Li, H. Li and Y. Wang, *Green Chem.*, 2015, **17**, 715.
29 S. C. Yan, Z. S. Li and Z. G. Zou, *Langmuir*, 2010, **26**, 3894.
30 Z. Jin, N. Murakami, T. Tsubota and T. Ohno, *Appl. Catal., B*, 2014, **150–151**, 479.
31 Y. Xu and W. D. Zhang, *Eur. J. Inorg. Chem.*, 2015, **2015**, 1744.
32 S. Hwang, S. Lee and J.-S. Yu, *Appl. Surf. Sci.*, 2007, **253**, 5656.
33 E. G. Gillan, *Chem. Mater.*, 2000, **12**, 3906.
34 V. N. Khabashesku, J. L. Zimmerman and J. L. Margrave, *Chem. Mater.*, 2000, **12**, 3264.
35 Q. Guo, Y. Xie, X. Wang, S. Zhang, T. Hou and S. Lv, *Chem. Commun.*, 2004, **1**, 26.
36 L. Ge and C. Han, *Appl. Catal., B*, 2012, **117–118**, 268.
37 Q. Xiang, J. Yu and M. Jaroniec, *J. Phys. Chem. C*, 2011, **115**, 7355.
38 Y. Yang, Y. Guo, F. Liu, X. Yuan, Y. Guo, S. Zhang, W. Guo and M. Huo, *Appl. Catal., B*, 2013, **142–143**, 828.
39 A. Thomas, A. Fischer, F. Goettmann, M. Antonietti, J. O. Muller, R. Schlogl and J. M. Carlsson, *J. Mater. Chem.*, 2008, **18**, 4893.
40 Y. He, Y. Wang, L. Zhang, B. Teng and M. Fan, *Appl. Catal., B*, 2015, **168–169**, 1.
41 P. Xiao, Y. X. zhao, T. Wang, Y. Y. Zhan, H. H. Wang, J. L. Li, A. Thomas and J. J. Zhu, *Chem.–Eur. J.*, 2014, **20**, 2872.